ISSN 1330-3651 (Print), ISSN 1848-6339 (Online) https://doi.org/10.17559/TV-20240301001359
Original scientific paper

Image Multi-Threshold Segmentation Based on Variable Precision Rough Set and K-L Roughness Particle Swarm Optimization

Zhiyong SHE*, Tao SONG, Dongpo ZHANG, Yueping FENG

Abstract: This paper proposes an image multi-threshold segmentation algorithm based on variable precision rough sets and K-L roughness particle swarm optimization. The algorithm does not require a priori knowledge outside the image and employs variable precision rough sets to address the uncertainty problem in image segmentation. The optimal segmentation threshold is obtained by combining K-L divergence and roughness, and an improved particle swarm optimization algorithm is used to enhance segmentation efficiency. Experimental results demonstrate that the proposed algorithm effectively solves the uncertainty problem in segmentation and achieves better segmentation performance compared to other algorithms.

Keywords: K-L roughness divergence; multi threshold segmentation; particle swarm optimization algorithm; variable precision rough set

1 INTRODUCTION

Image segmentation is to divide a complete image into several sets, there is no intersection between the sets, each set has special properties. At the beginning of image segmentation research, the image is usually divided into two parts: object and background. With the emergence of image multi-object tracking and optimization, only dividing an image into two parts can no longer meet the needs of subsequent image analysis and recognition. In recent years, many researchers have focused on the segmentation of images into multiple parts, that is, multi-object segmentation.

Multi-object segmentation based on traditional segmentation methods will greatly increase the number of iterations of image segmentation. Thus, the complexity of image segmentation is improved. In order to improve both segmentation accuracy and segmentation efficiency, many scholars have proposed some algorithms for multi-object segmentation of images. In terms of multi-object segmentation based on improved heuristic algorithms, Zhao Feng et al. proposed a threshold image segmentation algorithm based on hybrid optimization of multi-objective particle swarm optimization and artificial bee colony [1], and multi-population joint multi-objective evolutionary adaptive threshold image segmentation algorithm [2]. Fuqi Lv et al. proposed a multi-level threshold image segmentation algorithm based on particle swarm optimization algorithm and fuzzy entropy [3], Shang C et al. proposed a gradient-based multilevel thresholding method [4]. In terms of multi-object segmentation based on contour extraction method, Chen Hua et al. proposed a synthetic aperture radar (SAR) image target segmentation method based on boundary and texture information [5]. This method can effectively suppress coherent noise. The interference of image blobs and small targets is removed, the automatic target segmentation of SAR image is realized. Zhang Xinran et al. proposed the implementation of an algorithm for extracting the outer contour of head MRI images [6]. Fang L. et al. proposed a salient contour extraction method based on multi-level feature channel optimization coding [7]. In terms of multi-object segmentation based on neural network, Lu Wei et al. proposed the application of improved Mask R-CNN network in medical image recognition and segmentation [8], Liu Xiaoni et al. proposed a multi-objective image segmentation method based on FCM and discrete regularization [9], Tran V. L. et al. proposed a deep neural network for object semantic segmentation and 6D pose recognition [10].

However, the algorithms listed above cannot effectively solve the complexity of image in the process of multi-threshold segmentation, randomness and uncertainty. Variable precision rough set is an effective mathematical tool for dealing with randomness and uncertainty [11-14]. But as the threshold increases, the computational complexity of image segmentation based on variable precision rough set also increases. In this paper, an image multi-threshold segmentation algorithm based on variable precision rough set and K-L rough divergence particle swarm is proposed. It can effectively solve the above problems in image segmentation; at the same time, the segmentation accuracy and calculation efficiency are improved.

Multi-object segmentation is applied in many scenarios. For example, a one-step inductive multi-objective learning (OSAMTL-DiNS-) with different noise samples proposed by Y Yang et al. OSAMTL-DiNS is applied to tumor segmentation of breast cancer (TSfBC) [29]; a novel multi-target tracking and segmentation method proposed by MP Muresan et al., which is suitable for hot images and can track the object at the bounding box and instance mask level [30]; a GWO-SCE adaptive multi-threshold segmentation and subdomain fault method proposed by Y. Liu et al. [31]; a joint depth and depth for population object level segmentation and stereo tracking proposed by J. Li et al [32]. All the above are based on the application of target segmentation. An efficient and accurate multi-threshold segmentation algorithm is proposed to solve the uncertainty problem and improve the segmentation performance by combining variable precision coarse set, K-L divergence and improved particle swarm optimization algorithm. This method can quickly and highly perform target information segmentation in medical segmentation, multi-object tracking and scene comprehension. This method has important application value, contribution and application prospect in multi-object segmentation.

2. THEORETICAL BASIS

2.1 Variable Precision Rough Sets

Definition 1 Let set $X \subseteq U$ and $X \neq \varnothing$, $Y \subseteq U$ and $Y \neq \varnothing$, U is a finite set, If $\forall e \in X$, $\exists e \in Y$, be called $X \subseteq Y$.令

$$c(X,Y) = \begin{cases} 1-|X \bigcap Y|/|X|, |X|>0 \\ 0, |X|=0 \end{cases} \quad (1)$$

In this case, the misclassification rate of X and Y is $c(X,Y)$;令 $0 \le \beta < 0.5$. Majority inclusion relation is defined as $X \overset{\beta}{\subseteq} Y \Leftrightarrow c(X,Y) \le \beta$.

Definition 2 $S=(U,R)$ is the knowledge base, $U \neq \varnothing$, R is the upper equivalence relation of U, $U/R = \{E_1, E_2, E_3, \cdots, E_n\}$ is the underlying equivalence classification of R. For $X \subseteq U$, then the set of β lower approximations of X : $\underline{R}_\beta X = \bigcup \{E \in U/R \mid c(E,X) \le \beta\}$

The set of approximations on β of X : $\overline{R}_\beta X = \bigcup \{E \in U/R \mid c(E,X) < 1-\beta\}$

β accuracy of X : $\alpha(R,\beta,X) = \dfrac{|\underline{R}_\beta X|}{|\overline{R}_\beta X|}$

β roughness of X : $\rho(R,\beta,X) = 1-\alpha(R,\beta,X)$

Lemma 1 $\xi(R,X) = \max(m_1, m_2)$ Among them $m_1 = 1 - \min\{c(E,X) \mid E \in U/R, 0.5 < c(E,X)\}$, $m_2 = \max\{c(E,X) \mid E \in U/R, c(E,X) < 05\}$ [15].

2.2 K-L Divergence

In probability, K-L divergence is used to measure the similarity of two probability distributions P and Q, where P represents the probability distribution of the original dataset, Q is an approximate estimate of P. The K-L divergence also represents the amount of information loss when Q makes an approximate estimate of P [16-21].

Under $\alpha \in [0,1) \bigcup (1,\infty)$, let $P: x \to [0,1]$ and $Q: x \to [0,1]$ be two probability distributions, then the K-L divergence of P and Q can be expressed as:

$$D_\alpha(P \| Q) = \log\left[\left(\sum_x \frac{P(x)^\alpha}{Q(x)^{\alpha-1}} \right)^{\frac{1}{\alpha-1}} \right] \quad (2)$$

The smaller is the value of Eq. (2), then $D_\alpha(P \| Q)$ - divergence means that P and Q are closer together.

When $\alpha \to 1$, the limiting value $D_1(P \| Q) = \lim_{\alpha \to 1} D_\alpha(P \| Q)$ of this divergence is the same as in the following formula [22-28].

$$D(P \| Q) = \sum_x P(x) \log \frac{P(x)}{Q(x)} \quad (3)$$

K-L divergence Eq. (3). It is required that P and Q have the same dimension, and $\sum_{x_i} p(x_i) = \sum_{x_i} q(x_i)$. In image segmentation, let P be the image to be segmented, Q is the segmentation result map of the corresponding image.

2.3 Improved Particle Swarm Optimization Algorithm

The original particle Swarm optimization (PSO) is an iterative optimization algorithm, which consists of a swarm of particles. Each particle is defined as a location in space. The particles are initialized with a random set of solutions. Through iteration, the local optimal value is searched first, and then the global optimal value is obtained. When k particles fly in n -dimensional space searching for the optimal solution, each particle has two characteristic properties: velocity and position. The rate and position of the *j*-th component of the *i*-th particle are updated according to Eqs. (4) and (5), respectively.

$$v_{ij}(t+1) = \omega \times v_{ij}(t) + c_1 \times rand_1 \times (pBest_j(t) - x_{ij}(t)) + c_2 \times rand_2 \times (gBest_j(t) - x_{ij}(t)) \quad (4)$$

$$x_{ij}(t+1) = x_{ij}(t) + v_{ij}(t+1) \quad (5)$$

where ω, c_1, c_2, $pBest$, $gBest$ are inertial weights respectively, individual learning factor, the group learning factor, the global optimal solutions and local optimal solutions.

PSO has some defects such as premature convergence, fast convergence speed but easy to fall into local optimal solution, and poor combination. To this end, in this paper, the nonlinear factor fa to prevent premature convergence and the operator ga to help the particle escape the local optimal solution are proposed, as shown in Eqs. (6) and (7). The particle swarm optimization proposed in reference [24] also designs premature convergence linear factors. As a comparison algorithm, the particle swarm optimization algorithm is referred to as MPSO.

$$fa = rand \times (1 - e^{t-T}) \quad (6)$$

$$gBest_j = gBest_j + ga = gBest_j + (\max(x_j) - \min(x_j)) \times rand \quad (7)$$

In Eq. (6), t t is the current number of iterations, T is the total number of iterations. In Eq. (7), $\max(x_j) - \min(x_j)$ is the difference between the maximum and minimum positions of particles in each iteration,Is a random distribution among the $rand \in [0,1]$ occurrences in a particle swarm. In this paper, the improved particle swarm optimization algorithm is modified from Eq. (5) through Eq. (6), as shown in Eq. (8).

$$x_{ij}(t+1) = x_{ij}(t) + fa \times v_{ij}(t+1) \quad (8)$$

In this paper, the combination of K-L divergence and roughness, set roughness is taken as the objective function of multi-threshold segmentation mainly because: K-L divergence can measure the similarity between two things, and the larger the roughness, the greater the gap between the segmented image and the target image. In order to segment the image more accurately, K-L divergence is introduced to further improve the roughness. K-L roughness is the objective function to obtain more accurate segmentation threshold, and finally segment multiple objects in the image. In order to obtain the threshold of segmentation image quickly, this paper proposes the PSO of nonlinear escape factor, which not only improves the efficiency of acquisition threshold, but also can avoid the loss of important threshold, and can obtain the global optimal threshold, rather than the local optimal threshold. Therefore, the objective function with K-L roughness divergence as the nonlinear escape factor PSO can theoretically obtain multiple thresholds of excellent segmentation images and segment the image with multiple objectives.

3 PROPOSED ALGORITHM

In this paper, the image is represented by variable precision rough set. On this basis, the relationship between image variable precision rough set, divergence and image segmentation is analyzed. Explain the minimum K-L rough divergence as the objective function for finding the best multiple thresholds, and the objective function is derived. After that, the improved PSO was used to deal with the premature convergence and local optimal solution of the particle swarm. Finally, the K-L rough divergence is used as the fitness function of IPSO to solve the best multiple segmentation thresholds. Thus, the relationship between K-L rough divergence and the heuristic algorithm is established.

3.1 Variable Precision Rough Sets Represent Images

Variable precision rough set can effectively deal with randomness and uncertainty, and it is more accurate than classical rough set. In this paper, variable precision rough sets are used to represent images. Let the original graph F be an image of size $M \times N$. Its gray level is $0,1,\ldots L-1$ ($L=256$), every pixel of the original graph F is used to form a universe U. Partition the universe U into mutually disjoint subblocks of size $m \times n$. Among them $m \le M$, $n \le N$. Denote $K = M \times N / m \times n$ as the total number of partitioned sub-blocks, call each sub-block F_i ($i=1,2\ldots K$) a particle. After F particle of the image, multi-threshold segmentation is performed on the original image F. Let's say $m1$ has some threshold, denoted by $t_1, t_2, \ldots t_{m1}$ .Among them $t_1 < t_2 < \ldots < t_{m1}$, divide the original graph F into $m1+1$ classes, are respectively $B_1, O_1, O_2 \ldots, O_{m1}$. Then $B_1, O_1, O_2, \ldots, O_{m1}$ correspond to pixels with gray levels, $\{0,1,\ldots,t_1\}$, $\{t_1+1, t_1+2, \ldots, t_2\}$, $\{t_2+1, t_2+2, \ldots, t_3\}, \ldots, \{t_{m1}+1, t_{m1}+2, \ldots, L-1\}$ respectively. $f_{\max} F$ and $f_{\min}$ are the maximum and minimum pixel values of the original image, respectively.

Let set $X = \{f(P_j) \mid f(P_j) \le t_1\}$, $Y = \{f(P_j) \mid t_k < f(P_j) \le t_{k+1}\}$. According to Definition 2, the variable precision rough set representation of the background subgraph and the ml target subgraph of the original graph F of the segmentation result graph F' are determined as follows:

Segmentation result figure F' background lower approximation set, upper approximation set:

$$\underline{F'B}_{t_1} = \bigcup_{i=1}^{K} \{F_i' \mid c(F_i', X) \le \beta_{F'1}\}$$

$$\overline{F'B}_{t_1} = \bigcup_{i=1}^{K} \{F_i' \mid c(F_i', X) < 1-\beta_{F'1}\}$$

Lower approximation set, upper approximation set in the background of the original graph F :

$$\underline{FB}_{t_1} = \bigcup_{i=1}^{K} \{F_i \mid c(F_i, X) \le \beta_{F1}\}$$

$$\overline{FB}_{t_1} = \bigcup_{i=1}^{K} \{F_i \mid c(F_i, X) < 1-\beta_{F1}\}$$

Segmentation result figure F' Lower approximation set and upper approximation set of target set:

$$\underline{FO}_k = \bigcup_{i=1}^{K} \{F_i \mid c(F_i, Y) \le \beta_{Fi}\}$$

$$\overline{FO}_k = \bigcup_{i=1}^{K} \{F_i \mid c(F_i, Y) < 1-\beta_{Fi}\}$$

A key step in using variable precision rough set to represent an image is to determine the classification error $\beta \in [0,0.5)$. To this end, a series of classification errors of the segmentation result image F' the background subimage of the original image F , and the ml target subimages are solved according to Lemma 1.

$$\underline{F'O}_k = \bigcup_{i=1}^{K} \{F_i' \mid c(F_i', Y) \le \beta_{F'i}\}$$

$$\overline{F'O}_k = \bigcup_{i=1}^{K} \{F_i' \mid c(F_i', Y) < 1-\beta_{F'i}\}$$

A key step in using variable precision rough set to represent an image is to determine the classification error $\beta \in [0,0.5)$. To this end, a series of classification errors of the segmentation result image F' the background subimage of the original image F , and the ml target subimages are solved according to Lemma 1.

3.2 Construct the K-L Rough Divergence

According to the variable precision rough set theory, when the variable precision rough set is used to deal with classification problems, the smaller the roughness is, the more accurate the corresponding classification is. Accordingly, for the image represented by the variable precision rough set in Section 3.1, when the roughness of the segmentation result image F' , the background subimage of the original image F and the m_1 target subimages are smaller, the corresponding gray value classification is more accurate. The K-L divergence is a way to quantify the difference between two probability distributions P and Q. A smaller value of the divergence indicates a smaller error in the amount of information between the two distributions. Therefore, the K-L divergence can be used to measure whether the segmentation result image F' is accurate, and the roughness of the background subimage and m_1 object subimages of the segmentation result image and the original image is a probability value, which can also affect

the accuracy of the segmentation image. So, combining the roughness of the segmented image, the background sub-image of the original image and the m_1 target sub-images with the K-L divergence effectively, the accuracy of the segmented image can be better measured in theory, and the K-L rough divergence is obtained, the specific derivation is given below:

$$\rho_{F^{'}B_{t_1}} = 1 - \frac{|\underline{F^{'}B}_{t_1}|}{|\overline{F^{'}B}_{t_1}|}, \rho_{FB_{t_1}} = 1 - \frac{|\underline{FB}_{t_1}|}{|\overline{FB}_{t_1}|}$$

$$\rho_{F^{'}O_{t_k}} = 1 - \frac{|\underline{F^{'}O}_{t_k}|}{|\overline{F^{'}O}_{t_k}|}, \rho_{FO_{t_k}} = 1 - \frac{|\underline{FO}_{t_k}|}{|\overline{FO}_{t_k}|}$$

The K-L rough divergence is obtained from Eq. (3):

$$R(\mathrm{F} \| \mathrm{F}^{'}) = \sum_{t_k=t_1}^{t_m} (\rho_{F^{'}O_{t_k}} \log \frac{\rho_{F^{'}O_{t_k}}}{\rho_{FO_{t_k}}} + \rho_{F^{'}B_{t_1}} \log \frac{\rho_{F^{'}B_{t_1}}}{\rho_{FB_{t_1}}}) \quad (9)$$

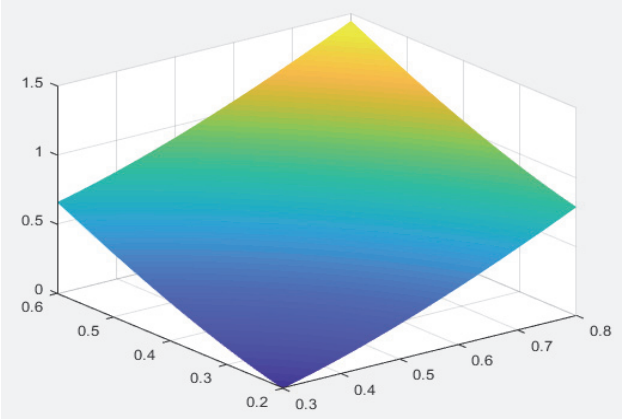

Figure 1 K-L roughness divergence surface

Fig. 1 shows a surface plot of the K-L rough divergence. The smaller the value of Eq. (9), the more accurate the image multi-threshold segmentation is. When Eq. (9) reaches the minimum value, the segmentation threshold is the best segmentation threshold. The expression is as follows:

$$\{t_1^*, t_2^*, t_3^*, \cdots, t_m^*\} = \min_{\{t_1^*, t_2^*, t_3^*, \cdots, t_m^*\}} R(\mathrm{F} \| \mathrm{F}^{'}) \quad (10)$$

Based on Eq. (10), the time complexity of solving the optimal threshold for image multi-threshold segmentation by ordinary iteration is $O((L-1)^{2n})$, where L is the maximum gray value of the image and n is the number of thresholds to segment the image. It can be seen that with the increase of the number of thresholds, the time complexity of solving the optimal segmentation threshold will show an exponential growth, resulting in low computational efficiency. In this case, the improved particle Swarm Optimization (IPSO) algorithm is used to improve the efficiency of solving the optimal segmentation threshold.

3.3 K-L Coarse Divergence Combined with IPSO

The process of IPSO to find the global optimal solution is equivalent to finding the best segmentation threshold for image multi-threshold segmentation. The m thresholds of image multi-threshold segmentation are treated as the m-dimensional space of IPSO.

The K-L rough divergence function is used as the fitness function of IPSO to find the optimal solution, and the segmentation threshold corresponding to the global optimal solution *gBest* is the optimal segmentation threshold. In this paper, the multiple threshold segmentation algorithm flow chart is shown in Fig. 2.

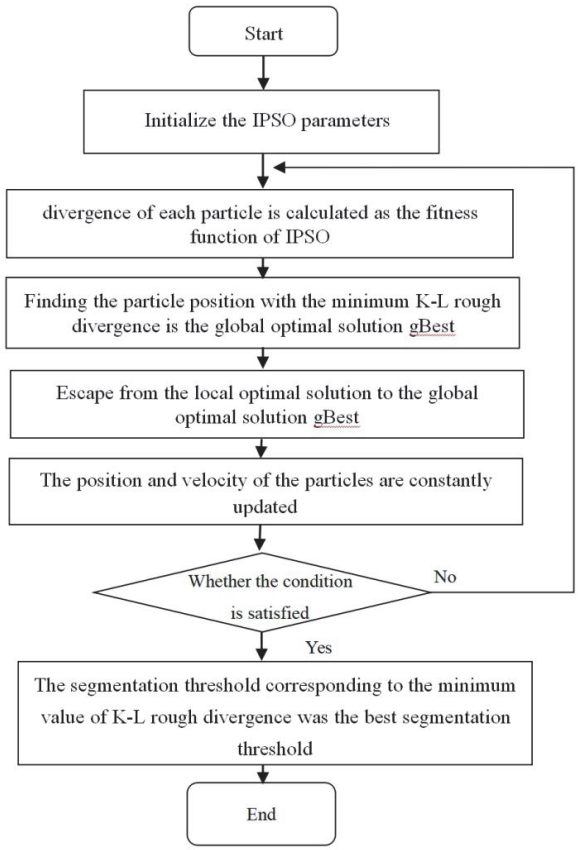

Figure 2 Flow chart of the proposed multi threshold segmentation algorithm

4 EXPERIMENTAL ANALYSIS

The experimental images come from the BSDS500 dataset, MATLAB R2018a was used for the experiments, 8G RAM in operation, Intel(R) Core(TM) i5-8250U CPU @ 1.60GHz, 1.80 GHz processor for image multi-threshold segmentation. The number of particles, individual learning factor, group learning factor and iteration times of IPSO were 20, 2.0, 2.0 and 200, respectively. Inertia weight $\omega = \omega_{\max} - (\omega_{\max} - \omega_{\min})/(1 - e^{t-T})$, the maximum and minimum inertia weights $\omega_{\max}, \omega_{\min}$ are fixed values of 0.9 and 0.1, respectively. Tabs. 1 and 2 show that IPSO, MPSO and PSO respectively use K-L rough divergence as fitness function to solve the function values corresponding to different iterations under 3 and 5 segmentation thresholds. Figs. 3a and 3b show the convergence plots of the fitness function for the three PSO algorithms with 3 and 5 segmentation thresholds, respectively.

From the data analysis of Tabs. 1, 2 and Figs. 3a and 3b, when the number of iterations is between 0 and 200, IPSO converges slower than MPSO and PSO. This is because although both IPSO and MPSO have *fa* factors,

the *fa* factor of IPSO is nonlinear and the *fa* factor of MPSO is linear.

IPSO will not ignore some important values and miss the relatively better segmentation threshold in the iterative process, resulting in a relatively slow convergence speed. The convergence rate of PSO is faster than that of IPSO and MPSO, which indicates that the *fa* factor will indeed prevent premature convergence of the PSO algorithm. After the number of iterations reaches 200, the values of the three particle swarm optimization algorithms almost no longer fluctuate, but the late convergence of MPSO and PSO is not as stable as IPSO, which indicates that the value of the fitness function obtained by MPSO and PSO is not as reliable as IPSO.

Table 1 3 Segmentation threshold iteration information

	10	20	30	40	...	90	100	110	120	...	160	170	180	190
IPSO	1.44	1.22	0.86	0.86	...	0.44	0.41	0.40	0.43	...	0.24	0.25	0.24	0.24
MPSO	1.33	0.72	0.66	0.50	...	0.38	0.40	0.31	0.32	...	0.29	0.32	0.25	0.24
PSO	0.55	0.36	0.34	0.30	...	0.30	0.16	0.19	0.27	...	0.19	0.20	0.18	0.20

Table 2 5 Segmentation threshold iteration information

	10	20	30	40	...	90	100	110	120	...	160	170	180	190
IPSO	1.25	0.94	0.73	0.63	...	0.30	0.27	0.22	0.22	...	0.17	0.16	0.17	0.16
MPSO	0.91	0.41	0.25	0.17	...	0.16	0.16	0.18	0.16	...	0.17	0.17	0.17	0.17
PSO	0.27	0.16	0.14	0.13	...	0.13	0.14	0.14	0.13	...	0.17	0.13	0.13	0.13

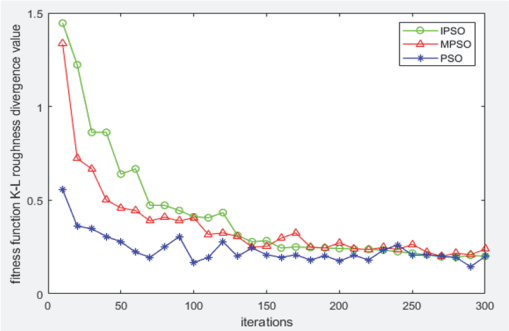

Figure 3a 3 convergence diagram of threshold fitness function

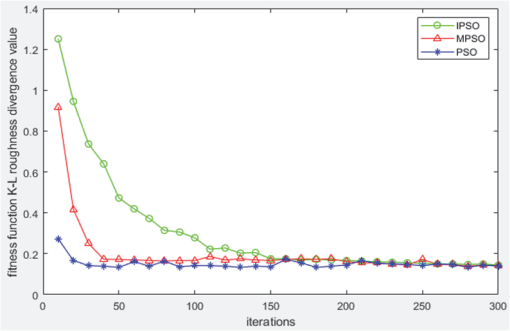

Figure 3b 5 convergence diagram of threshold fitness function

The next experiment takes four images from the BSDS500 dataset. The proposed algorithm, MPSO-K-L divergence, PSO-maximum rough entropy and PSO-maximum entropy algorithms were used to perform 3-threshold and 5-threshold segmentation respectively. The optimal objective function value obtained by segmentation and the corresponding optimal segmentation threshold and other quantity values are shown in Tabs. 3 and 4.

$|\overline{\beta}_0| \in [0, 0.5)$ in Tabs. 3 and 4, is the average of the classification error of the target subgraph. The two figures in Figs. 4a and 4b show the average classification error in the iterative process under the 3-threshold segmentation and the 5-threshold segmentation, respectively, corresponding to the objective function values of Eq. (9). As can be seen from the figure, for both 3-threshold segmentation and 5-threshold segmentation, as $|\overline{\beta}_0|$ decreases, the value of Eq. (9) also decreases. This is because $|\overline{\beta}_0|$ is the main factor affecting the value of Eq. (9). The smaller the value of Eq. (9), the smaller the error between the segmented image and the original image information, the better the corresponding segmentation threshold, and the better the segmentation effect. In the theory of variable precision rough set, the smaller the classification error is, the more accurate the classification is. The experimental results show that the best segmentation threshold can be obtained by using variable precision rough set to represent the image.

Table 3 Values of each quantity of threshold segmentation

Image	Algorithm	Subgraph	Number of convergence	Objective function value	Optimal segmentation threshold	$\overline{\beta}_0$
480 × 480	Algorithm in this paper	8 × 8	160	0.0206	42, 128, 187	0.2596
	MPSO-K-Ldivergence algorithm	--	180	0.0898	52, 95, 142	--
	PSO-maximum rough entropy algorithm	8 × 8	200	15.1409	66, 129, 182	--
	PSO-Maximum Entropy algorithm	--	200	10.6254	68, 130, 184	--
720 × 720	Algorithm in this paper	8 × 8	165	0.0530	49, 113, 208	0.2720
	MPSO-K-Ldivergence algorithm	--	190	0.1115	54, 86, 118	--
	PSO-maximum rough entropy algorithm	8 × 8	200	22.4281	83, 156, 219	--
	PSO-Maximum Entropy algorithm	--	200	14.6085	81, 154, 210	--
560 × 560	Algorithm in this paper	8 × 8	160	0.0311	40, 129, 202	0.3019
	MPSO-K-Ldivergence algorithm	--	185	0.1239	80, 150, 183	--
	PSO-maximum rough entropy algorithm	8 × 8	200	15.1259	75, 147, 186	--
	PSO-Maximum Entropy algorithm	--	200	10.5318	38, 83, 185	--
400 × 400	Algorithm in this paper	8 × 8	150	0.0437	52, 112, 225	0.2901
	MPSO-K-Ldivergence algorithm	--	175	0.7661	51, 108, 204	--
	PSO-maximum rough entropy algorithm	8 × 8	200	15.5137	95, 153, 204	--
	PSO-Maximum Entropy algorithm	--	200	10.6150	97, 161, 204	--

Table 4 5 Values of each quantity of segmentation threshold

Image	Algorithm	Subgraph	Number of convergence	Objective function value	Optimal segmentation threshold	$\overline{\beta}_0$
480 × 480	Algorithm in this paper	8 × 8	160	0.0101	42, 128, 181, 187, 235	0.2601
	MPSO-K-Ldivergence algorithm	--	180	0.0656	36, 65, 96, 142, 191	--
	PSO-maximum rough entropy algorithm	8 × 8	200	20.9785	52, 95, 139, 183, 219	--
	PSO-Maximum Entropy algorithm	--	200	15.6771	31, 52, 74, 95, 142	--
720 × 720	Algorithm in this paper	8 × 8	165	0.0204	49, 113, 208, 204, 234	0.2853
	MPSO-K-Ldivergence algorithm	--	190	0.0757	59, 95, 138, 175, 219	--
	PSO-maximum rough entropy algorithm	8 × 8	200	20.3974	62, 97, 136, 178, 216	--
	PSO-Maximum Entropy algorithm	--	200	15.5403	59, 94, 134, 172, 214	--
560 × 560	Algorithm in this paper	8 × 8	160	0.0204	40, 129, 202, 190, 238	0.3015
	MPSO-K-L divergence algorithm	--	185	0.0642	32, 63, 91, 119, 149	--
	PSO-maximum rough entropy algorithm	8 × 8	200	21.0970	36, 76, 115, 149, 185	--
	PSO-Maximum Entropy algorithm	--	200	15.6330	34, 62, 91, 120, 150	--
400 × 400	Algorithm in this paper	8 × 8	150	0.0321	52, 112, 225, 203, 235	0.2905
	MPSO-K-L divergence algorithm	--	175	0.0810	39, 89, 126, 161, 204	--
	PSO-maximum rough entropy algorithm	8 × 8	200	21.1943	47, 91, 128, 161, 203	--
	PSO-Maximum Entropy algorithm	--	200	15.7856	53, 94, 129, 167, 202	--

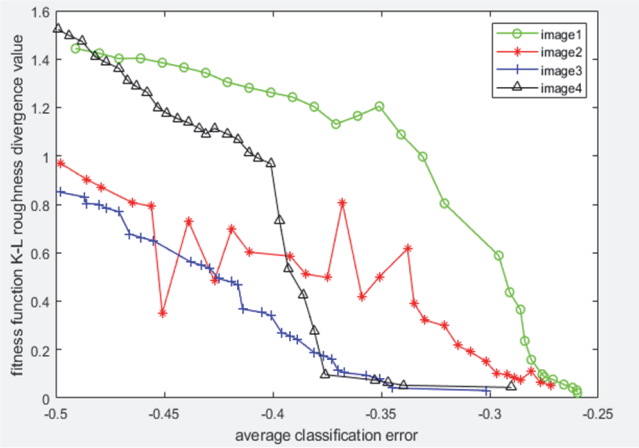

Figure 4a 3 Corresponding diagram of division and Eq. (9)

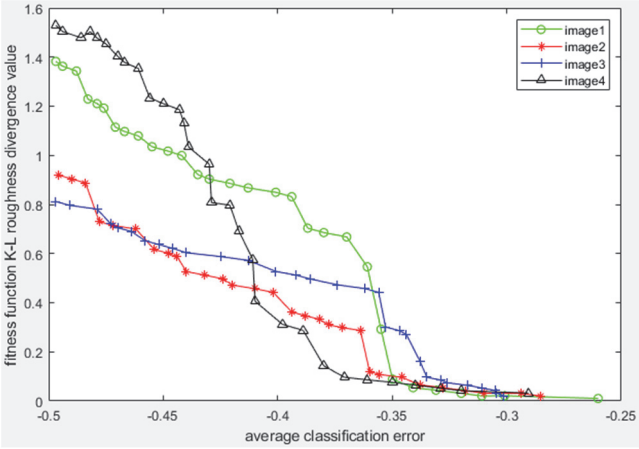

Figure 4b 5 Corresponding diagram of division and Eq. (9)

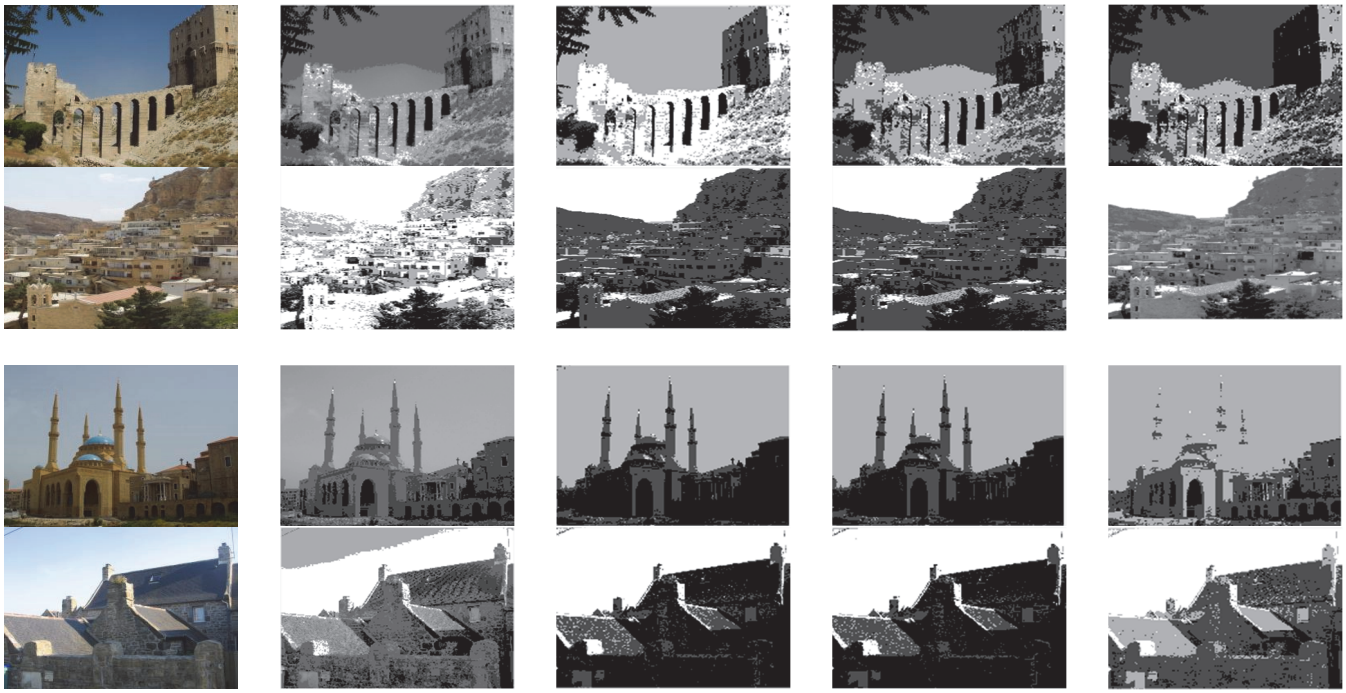

(a) (b) (c) (d) (e)

Figure 5 Comparison of 3-threshold segmentation of the proposed algorithm and the other three algorithms.(a) Original image (b) Segmentation algorithm in this paper (c) MPSO-K-L divergence algorithm (d) PSO-maximum rough entropy algorithm (e) PSO-Maximum Entropy algorithm

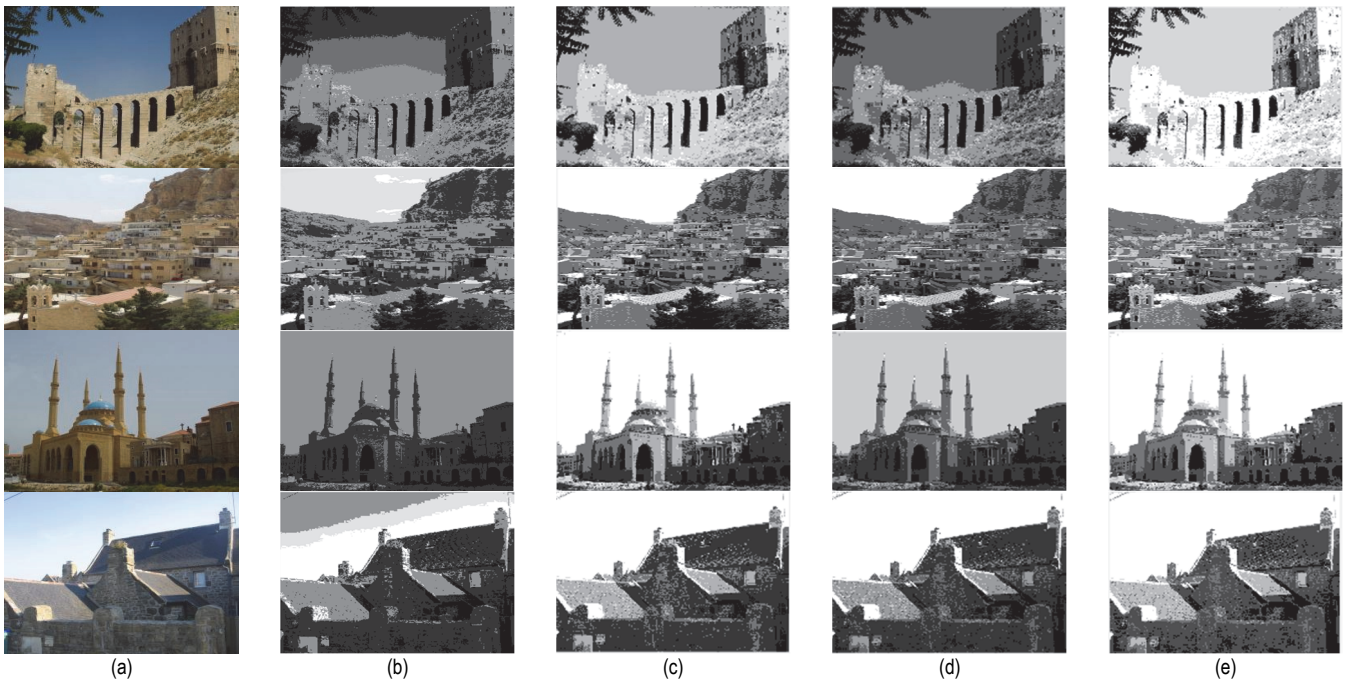

Figure 6 Comparison of 5-threshold segmentation between the proposed algorithm and the other three algorithms. (a) Original image (b) Segmentation algorithm in this paper (c) MPSO-K-Ldivergence algorithm (d) PSO-maximum rough entropy algorithm (e) PSO-maximum rough entropy algorithm

Figs. 5 and 6 show the effects of the above 3-threshold and 5-threshold segmentation respectively, where (a) is the original image, and (b), (c), (d), and (e) are the final segmentation effects.

For the 3-threshold segmentation, in the first image of Fig. 5b, the segmentation outline of the building behind the background is clear, while the outline of the building is not visible in (c), (d), and (e); in the third image of (b), the right building contour segmentation is clearly visible, while the right buildings of (c), (d), and (e) are not segmented out. For 5-threshold segmentation, in the first image of Figs. 6b, the levels of sky blue change are clearly segmented, while (c), (d), and (e) are not. In the second picture of (b), the window segmentation of the building under the mountain is very clear, while the contour of the segmented window in (c), (d), and (e) is not clear. Therefore, it can be seen from the segmentation effect that the proposed multi-threshold segmentation algorithm is better than the other three multi-threshold segmentation algorithms.

Table 5 Multi threshold segmentation efficiency of this algorithm for the same and different size images

Image	2-threshold value	3-threshold value	4-threshold value	5-threshold value
269 × 201	0.1567 s	0.1811 s	0.2451 s	0.3995 s
403 × 302	0.1776 s	0.2050 s	0.2804 s	0.4325 s
576 × 432	0.1996 s	0.2638 s	0.3581 s	0.5016 s
720 × 580	0.2185 s	0.3335 s	0.4319 s	0.6120 s

Tab. 5 show the time required by the proposed algorithm when segmenting images of different sizes with 2-threshold, 3-threshold, 4-threshold and 5-threshold, respectively. This table shows that the time complexity of the proposed segmentation algorithm is related to the number of segmentation thresholds and the image size. It can be seen from the table that under the same segmentation threshold, the time required for segmentation gradually increases as the image size increases. Similarly, in the same size image, with the increase of segmentation threshold, the time required for segmentation also increases, but the increase of time is not large. This is because the improved IPSO algorithm in this paper regards *n*-dimensional space as the multi-threshold of image segmentation, and uses the parallel ability of the algorithm to solve the best segmentation threshold in the calculation, and does not carry out iterative search one by one.

5 CONCLUSIONS

This paper introduces an image multi-threshold segmentation algorithm that combines variable precision rough sets, K-L roughness divergence, and an improved particle swarm optimization algorithm. The variable precision rough set representation of the image effectively addresses the uncertainty problem in segmentation, while the K-L rough divergence serves as an objective function to obtain the optimal segmentation threshold. The improved particle swarm optimization algorithm, with its nonlinear and escape factors, prevents premature convergence and local optima, significantly enhancing segmentation efficiency. Experimental results on the BSDS500 dataset validate the effectiveness and robustness of the proposed algorithm. The algorithm achieves better segmentation performance compared to other multi-threshold segmentation algorithms, particularly in terms of preserving object boundaries and handling complex scenes. The time complexity analysis further demonstrates the efficiency of the algorithm, showing a moderate increase in segmentation time with increasing image size and segmentation thresholds. However, there are still some limitations and future research directions to be addressed. The current study requires the number of segmentation thresholds to be set in advance, and an adaptive selection of the optimal number of thresholds could be explored. Additionally, the performance of the proposed algorithm on a wider range of image types and applications, such as medical images or remote sensing data, could be investigated to assess its generalizability.

In conclusion, the image multi-threshold segmentation algorithm proposed in this paper offers a promising solution for accurate and efficient multi-object segmentation. By effectively combining variable precision rough sets, K-L roughness divergence, and an improved particle swarm optimization algorithm, the algorithm addresses the uncertainty problem in segmentation and achieves superior performance compared to other methods. With further refinements and extensions, this algorithm has the potential to contribute to various image processing applications that require accurate and efficient multi-object segmentation.

6 REFERENCES

[1] Feng, Z., Grun, K. L., & Ni, M. J. (2020). Image segmentation algorithm based on hybrid optimization of multi-objective particle swarm optimization and artificial bee colony. *Computer Engineering and Science*, *42*(02), 281-290. https://doi.org/CNKI:SUN:JSJK.0.2020-02-013

[2] Feng, Z., Yue, Z., & Jun, W. (2018). Multi-objective evolutionary adaptive threshold image segmentation algorithm based on multi-population joint. *Application Research of Computer Science*, *35*(06), 1858-1862. https://doi.org/10.3969/j.issn.1001-3695.2018.06.058

[3] Qi, L. F. & Min, L. X. (2019). Multi-level threshold image segmentation algorithm based on particle swarm optimization algorithm and fuzzy entropy. *Computer Application Research*, *36*(09), 2856-2860. https://doi.org/10.19734/j.issn.1001- 3695.2018.04.0236

[4] Shang, C., Zhang, D., &Yang, Y. (2021). A gradient-based method for multilevel thresholding. *Expert Systems with Applications*, *175*(1),114845. https://doi.org/10.48550/arXiv.2105.13954

[5] Ran, Z. X., Ru, C. Q., & Jia, H. X. (2013). Implementation and comparison of external contour extraction algorithm of head MRI images. *Computer Applications and Software*, *30*(05), 11-14. https://doi.org/10.3969/j.issn.1000-386x.2013.05.004

[6] Hua, C., Wei, G., & Wen, Y. J. (2019). Synthetic aperture Radar image target segmentation based on boundary and texture information.*Chinese Journal of Image and Graphics*, *24*(06), 882-889. https://doi.org/CNKI:SUN:ZGTB.0.2019-06-004

[7] Fang, L. & Fan, Y. (2021). Saliency Contour Extraction Based on Multi- level Feature Channel Optimization Coding. *Electronics Science Technology and Application*, *7*(4), 117. https://doi.org/10.18686/esta.v7i4.168

[8] Wei, L., Dan, L., & Min, S. (2020). Application of Improved Mask R-CNN Network in Medical Image Recognition and Segmentation. *Computer Engineering and Applications*,1-8. https://doi.org/10.3778/j.issn.1002-8331.2105-0092

[9] Ni, L. X., Nan, L. Y., & Ling, L. (2015). Multi-objective image segmentation based on FCM and discrete regularization. *Journal of Computer Aided Design and Computer Graphics*, *27*(01), 142-146. https://doi.org/10.3969/j.issn.1003-9775.2015.01.018

[10] Tran, V. L. & Lin, H. Y. (2020). BiLuNetICP: A Deep Neural Network for Object Semantic Segmentation and 6D Pose Recognition. *IEEE Sensors Journal*, *PP*(99), 1-1. https://doi.org/10.1109/JSEN.2020.3035632

[11] Yong, S. Z., Chao, D., & Lei, Z. (2019). Image segmentation algorithm based on variable precision least square rough entropy.*Computer Engineering and Science*, *41*(04),657-664. https://doi.org/CNKI:SUN:JSJK.0.2019-04-013

[12] Nguyen, T. T., Wang, H. J., & Dao, T. K. (2020). A Scheme of Color Image Multithreshold Segmentation Based on Improved Moth-Flame Algorithm. *IEEE Access*, *8*, 174142-174159. https://doi.org/10.1109/ACCESS.2020.3025833

[13] Bin, Y., Yan, H., & Yun, K. (2023). A novel variable precision rough set attribute reduction algorithm based on local attribute significance.*International Journal of Approximate Reasoning*, *157*, 88-104. https://doi.org/10.1016/j.ijar.2023.03.002

[14] Hu, X., Jia, H., & Zhang, Y. (2023). An Open-Circuit Faults Diagnosis Method for MMC Based on Extreme Gradient Boosting. *IEEE Transactions on Industrial Electronics*. https://doi.org/10.1109/TIE.2022.3194584

[15] Shang, Z. W., Li, T. W., & Shu, Y. G. (2023). Neighborhood rough set with neighborhood equivalence relation for feature selection. *Knowledge and Information Systems*, *66*(3), 1833-1859. https://doi.org/10.1007/S10115-023-01999-Z

[16] Gong, Q., Zhao, X., & Bi, C. (2020). Maximum entropy multi-threshold image segmentation based on improved particle swarmoptimization. *Journal of Physics: Conference Series*, *1678*(1), 012098(9pp). https://doi.org/10.1088/1742-6596/1678/1/012098

[17] Yao, C., & Si, C. (2020). Application research of dynamic weight bat algorithm in image segmentation.*Computer engineeringand application*, *56*(14), 207-215. https://doi.org/10.3778/j.issn.1002-8331.2001-0310

[18] Jun, L., Song, Y. Y., & Yu, S. B. (2019). Two-dimensional Otsu multi-threshold image segmentation based on hybrid whale optimization algorithm. *Journal of Electronics and Information Technology*, *41*(08), 2017-2024. https://doi.org/10.11999/JEIT180949

[19] Wenying, Z., Min, D., & Li, J. (2023). Image segmentation using convolutional neural networks in multi-sensor information fusion. *Soft Computing*, *27*(23), 18353-18372. https://doi.org/10.1109/ACCESS.2019.2958330

[20] Hussein, D. & Bhat, G. (2023). SensorGAN: A Novel Data Recovery Approach for Wearable Human Activity Recognition. *ACM Transactions on Embedded Computing Systems*. https://doi.org/10.1145/3609425

[21] Bai, Y., Durand, J. B., & Forbes, F. (2023). Semantic segmentation of sparse irregular point clouds for leaf/wood discrimination. *ArXiv*, abs/2305.16963. https://doi.org/10.48550/arXiv.2305.16963

[22] Wang, Y. (2020). Otsu Image Threshold Segmentation Method Based on Seagull Optimization Algorithm. *Journal of Physics Conference Series*, *1650*, 032181. https://doi.org/10.1088/1742-6596/1678/1/012098

[23] Ewees, A. A. & Elaziz, M. A. (2020). Improved Artificial Bee Colony Using Sine-Cosine Algorithm for Multi-level Thresholding Image Segmentation. *IEEE Acces*, *PP*(99), 1-1. https://doi.org/10.1109/ACCESS.2020.2971249

[24] Lin, Q. Q., Zhang, L., & Wu, T. L. (2020). Application of Tsallis Cross-entropy in Image Thresholding Segmentation. *Sensors and Materials*, *32*(8), 2771. https://doi.org/10.18494/SAM.2020.2798

[25] Xu, J., Xu, L., & Gao, Z. (2020).A Denoising Method Based on Pulse Interval Compensation for High-Speed Spike-Based Image Sensor. *IEEE Transactions on Circuits and Systems for Video Technology*, *PP*(99), 1-1. https://doi.org/10.1109/TCSVT.2020.3034649

[26] Wei, Y.C., Lai, Y. X., & Su, H. P. (2020). Detecting Online Game Malicious Chargeback by using k-NN. *2020 IEEE 19th International Conference on Trust*, *Security and Privacy in Computing and Communications (TrustCom)*, 1971-1976. https://doi.org/10.1109/TrustCom50675.2020.00269

[27] Dongnian, J., Wei, L., & Fuyuan, S. (2020). Incipient fault diagnosis and amplitude estimation based on K-L divergence with a Gaussian mixture model. *The Review of scientific instruments*, *91*(5), 055103. https://doi.org/10.1063/5.0003535

[28] Markechová, D. & Riečan, B. (2019). K-L Divergence, entropy and mutual information of experiments in the intuitionistic fuzzy case. *Journal of Intelligent Fuzzy Systems*, *36*(4), 3857-3867. https://doi.org/10.3233/JIFS-18053

[29] Yang, Y., L, F., & Wei, Y. (2024). One-step abductive multi-target learning with diverse noisy samples and its application to tumor segmentation for breast cancer. *Expert Systems with Applications*, 251. https://doi.org/10.1016/j.eswa.2024.123923
[30] Muresan, M.P., Danescu, R., & Nedevschi, S. (2023). Multi-Object Tracking, Segmentation and Validation in Thermal Images. *IEEE Intelligent Vehicles Symposium (IV)*, 1-8. https://doi.org/10.1109/IV55152.2023.10186655
[31] Liu, Y., Kang, J., & Wen, L. (2023). Fault Diagnosis Algorithm of Gearboxes Based on GWO-SCE Adaptive Multi-Threshold Segmentation and Subdomain Adaptation. *Processes*. https://doi.org/10.3390/pr11020556
[32] Li, J., Wei, L., & Zhang, F. (2019). Joint Deep and Depth for Object-Level Segmentation and Stereo Tracking in Crowds. *IEEE Transactions on Multimedia*, 2531-2544. https://doi.org/10.1109/TMM.2019.2908350

Contact information:

Zhiyong SHE, Master Lecturer
(Corresponding author)
Information Network Security College of Xinjiang University of Political Science and Law, Tumxuk Xinjiang, 844000, P. R. China;
No. 52 Qianhai East Street, Tumushuk City, Xinjiang
E-mail: szy@xjzfu.edu.cn

Tao SONG, Master Lecturer
School of Intelligence Technology, Geely University of China,
Chengdu Sichuan, 610000, P. R. China;
No. 123, SEC. 2, Chengjian Avenue, Eastern New District,
Chengdu City, Sichuan Province
E-mail: songtao@guc.edu.cn

Dongpo ZHANG, Master Lecturer
Information Network Security College of Xinjiang University of Political Science and Law, Tumxuk Xinjiang, 844000, P. R. China;
No. 52 Qianhai East Street, Tumushuk City, Xinjiang
E-mail: szy@xjzfu.edu.cn

Yueping FENG, Doctoral Professor
School of Computer Science and Technology, Jilin University,
Changchun, 130012, P. R. China;
No. 2699 Qianjin Street, Changchun City, Jilin Province
E-mail: fengyp@jlu.edu.cn